Journal of Alloys and Compounds 638 (2015) 334–343

Contents lists available at ScienceDirect

Journal of Alloys and Compounds

journal homepage: www.elsevier.com/locate/jalcom

Small polaron conduction in lead modified lanthanum ferrite ceramics

K.K. Bhargav, S. Ram, S.B. Majumder *

Materials Science Centre, Indian Institute of Technology, Kharagpur 721302, India

ARTICLE INFO

Article history:
Received 22 December 2014
Received in revised form 14 February 2015
Accepted 25 February 2015
Available online 19 March 2015

Keywords:
Orthoferrites
Auto-combustion
Polaron conduction
Dielectric and impedance spectroscopy

ABSTRACT

In the present work we have illustrated the physics of the electrical characteristics of nanocrystalline $La_{1-x}Pb_xFeO_3$, ($0 \leqslant x \leqslant 0.2$) powder prepared using auto-combustion synthesis. The effect of lead doping on the dielectric, impedance and ac conductivity characteristics of lanthanum ferrite has systematically been investigated. The synthesized powders were phase pure and crystallized into centrosymmetric Pnma space group. As compared to pure $LaFeO_3$ ceramics (dielectric constant ~ 14,000), the dielectric constant is grossly increased (~30,000) in Pb doped $LaFeO_3$. The temperature dependence of dielectric constant of 10.0 at.% Pb doped $LaFeO_3$ exhibits dielectric maxima similar to that observed in ferroelectric ceramics with non-centrosymmetric point group. For $La_{0.8}Pb_{0.2}FeO_3$ ceramics, the frequency dependence of the dielectric constant and loss tangent at various temperatures (300–450 K) exhibit typical colossal dielectric constant (CDC) like behavior. From the impedance spectroscopy we have estimated the grain and grain boundary resistance and capacitance of Pb doped $LaFeO_3$ that follow a small polaron hopping conduction model. Long range movement of the charge carriers govern the CDC behavior.

1. Introduction

Materials exhibiting a colossal dielectric constant (CDC with dielectric constant typically more than 10^4) are technically important for capacitative element based random access memories. $LaFeO_3$ ceramics have been reported to exhibit colossal dielectric constant with weak temperature dependence, and multiferroic characteristics [1–3]. Thus, similar to that found in $CaCu_3Ti_4O_{12}$, Chen et al. [4] reported colossal dielectric behavior of $LaFeO_3$ in the temperature range 80–315 K. Being strongly correlated electron system, the structure, magnetic, and electronic transport of transition metal oxide based orthoferrites are directly related to localized 3d electrons on transition metal cations. Lanthanum transition metal based orthoferrites have been considered very attractive, as the transport behavior can be tuned by suitable substitution of various impurity ions into the A and B sites of these orthoferrites [5–9]. The dielectric characteristics, polarization ordering, and electrical transport behavior of most of these orthoferrites remain poorly understood [10–14]. Additionally, orthorhombically distorted perovskite $LaFeO_3$ was found to be canted antiferromagnetic oxide [15,16] and charge-transfer (C–T) type insulator [17]. It remains unclear how the dielectric relaxation and polarization ordering changes with cation doping eat A (La) site.

We have systematically studied the phase formation behavior, microstructure, electrical, magnetic, and magnetodielectric characteristics of $LaFeO_3$ powders. As a typical application of these powders recently we have reported their low temperature butane sensing characteristics [18]. The electrical properties of nanocrystalline $LaFeO_3$ ceramics (ABO_3 type perovskite) can be tuned by aliovalent Pb^{2+} doping replacing La^{3+} at A site [19,20]. In the present paper we have systematically studied the phase formation behavior, microstructure and electrical characteristics of Pb^{2+} modified $LaFeO_3$ ceramics. The role played by the dopant cation/(s) in controlling the dielectric relaxation, electrical transport, and polarization ordering characteristics of these ceramics are illustrated.

2. Experimental

Using a modified Pechini process we have prepared lanthanum ferrite sol using lanthanum and iron nitrate as precursors. The details of the powder synthesis have been reported in our earlier publication [18]. To prepare $La_{1-x}Pb_xFeO_3$ ($0 \leqslant x \leqslant 0.2$) sol, stoichiometric precursor salts (lanthanum, lead and iron nitrate) are first dissolved in distilled water through continuous stirring. Then the aqueous solution of citric acid (C.A) (C.A: total cation (mole) ~1.5) and ethylene glycol (E.G.) (E.G.: C.A (mole) ~3) are added to the mixed precursor solution to form a polymer-metal cation network. Citric acid consists of three carboxyl groups and one hydroxyl group. It is a weak acid and easily decomposes in aqueous solution to its conjugate base which acts as chelating agent to trap the cations of precursor materials. In this process cations are first bonded by citric acid followed by a temperature assisted hydrolysis reaction of citric acid with ethylene glycol to form an internal ester linkage. The complex precursor sol is stirred for 4 h at 80 °C and finally cooled down to room temperature to prepare lead modified lanthanum ferrite sol. In order to

---

* Corresponding author. Tel.: +91 9433611775.
E-mail address: subhasish@matsc.iitkgp.ernet.in (S.B. Majumder).

http://dx.doi.org/10.1016/j.jallcom.2015.02.186
0925-8388/© 2015 Elsevier B.V. All rights reserved.

prepare lanthanum lead ferrite nano-particles, the sol is dried for few hours at 120 °C to evaporate the liquid content and to produce a gelled mass. The gel is heated at about 140 °C until the auto combustion is initiated. The combustion process includes the decomposition and auto-combustion of gel followed by the formation of dried $La_{1-x}Pb_xFeO_3$ ($0 \leqslant x \leqslant 0.2$) particles. The auto-combustion is considered as a thermally induced redox reaction in which the carboxylic group acts as reducing agent and nitrate ion (NO_3^-) plays the role of oxidant. Citric acid and ethylene glycol serve the role of organic fuel in this auto-combustion process. Since the process is completed within a very short period, the particle size of the synthesized powders remains in the nano-size regime. The auto-combusted powders were calcined at 700 °C for 2 h in air for the removal of residual organics and improve their crystallinity. The phase formation behavior and microstructural characteristics of the auto-combusted and calcined powders are characterized by Rietveld refinement analyses of the respective X-ray diffraction (Cu K_α radiation) pattern and electron microscopy respectively. For electrical measurements the calcined powders were compacted into circular pellet (diameter 8 mm, thickness 0.8 mm) and sintered at 950 °C for 2 h. The sintered pellets were electrode with silver paste for electrical measurements. A LCR meter (HIOKI 3532-50 HiTester, Japan and N4L PSM 1735, UK) interfaced to a PC was used to measure the capacitance, loss tangent, and impedance as a function of frequency in the temperature range of 150–600 K.

3. Results

3.1. Thermal analysis of as dried $LaFeO_3$ powders

Fig. 1 shows the TG, DTG, and DTA plots of a $LaFeO_3$ nano-powder so obtained in the temperature range 30–950 °C. The typical TG curve reveals a mass-loss $\Delta M_1 = 8.6\%$ in the region BCDE, before a value $\Delta M_0 = 1.8\%$ on desorption of moisture at early temperatures, when a residual carbon burns out on reheating an as-burnt powder. Small ΔM_1-value ensures that a solution precursor with metal nitrates and citric acid (fuel) burns out spontaneously in the organic species as gases from $LaFeO_3$ as a dried powder. 75–85% of this bonded carbon escapes as oxide quickly in a sharp peak in the first derivative curve (DTG) at 380 °C. This much temperature is attained easily when a precursor gel is fired in air, implying that a phase $LaFeO_3$ has formed during the primary combustion process. Part of the carbon that bonds to the $LaFeO_3$ directly in a surface layer relieves over higher temperatures 400–675 °C in the DE region with a weak DTG peak as early as 600 °C. After point E, the sample rather gains a small mass $\Delta M_2 = 0.6\%$, possibly in oxidizing the surface species that were reduced in a reaction with carbon at lower temperatures. The cations at the nascent surfaces that suffer from incomplete coordination in oxygen ions in the polygons recover upon the crystallites grow on heating in air. There are two exothermic peaks at ~280 and 440 °C, in which the former peak may be due to a removal of organics, while the latter indicates the crystallization of amorphous powder.

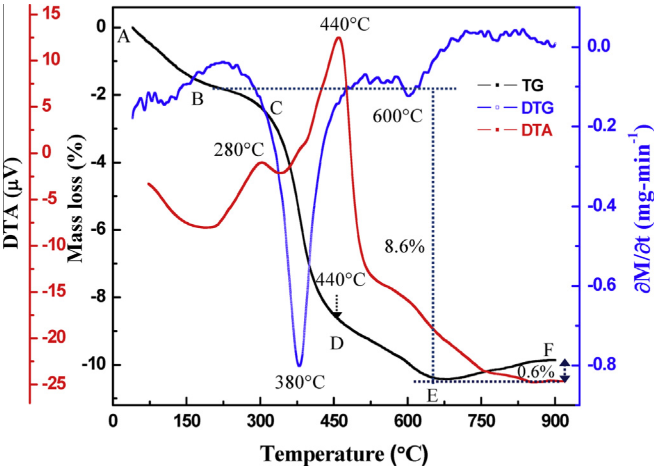

Fig. 1. TG, DTG and DTA characteristics of as-dried $LaFeO_3$ powder.

3.2. Phase formation and surface morphology of undoped and lead modified $LaFeO_3$ powders

Fig. 2(A) shows the X-ray diffractograms of (i) $LaFeO_3$ (LFO), (ii) 10.0 at.%, and (iii) 20.0 at.% Pb doped LFO powders calcined at 700 °C for 2 h in air. Fig. 2(B) shows slow scanned (1 2 1) diffraction peak showing a systematic shift indicating the change in lattice parameter with lead doping. Assuming orthorhombic *Pnma* space group we have performed the Rietveld refinements of these X-ray diffractograms and the refined patterns are shown as solid line in respective figures. Analyzing these XRD patterns it is apparent that auto-combustion synthesis is very effective to synthesize phase pure undoped and Pb doped $LaFeO_3$ powder at relatively lower calcinations temperature. The refined structural parameters are tabulated in Table I. Since cation radii of Pb^{2+} (~1.32 Å) is larger than La^{3+} (~1.15 Å), the lattice parameter is marginally increased in 10.0 at.% Pb doped powder, however, with further increase of the doping contents the lattice parameters changed marginally. As shown in the Table I, Pb^{2+} ion as *A* site dopant, significantly increases the crystallite size of LPFO powder and the theoretical density is marginally decreased.

The upper panel of Fig. 3 shows the FESEM micrographs of (a) $LaFeO_3$, (b) $La_{0.9}Pb_{0.1}FeO_3$, (c) $La_{0.8}Pb_{0.2}FeO_3$ powder calcined at 700 °C for 2 h in air. As shown in the figure, for pure $LaFeO_3$, as well as for 10.0 and 20.0 at.% Pb doped $LaFeO_3$ powders, it seems that the fine nano-crystalline primary particles are loosely sintered to form larger spherical shaped secondary particles. It yields meso-porous regions between primary particles and micro-porous regions between secondary particles. These powders were pressed and sintered at 950 °C for 2 h in air for electrical measurements. The lower panel of Fig. 3 shows the fractured FESEM micrographs of (d) $LaFeO_3$, (e) $La_{0.9}Pb_{0.1}FeO_3$, and (f) $La_{0.8}Pb_{0.2}FeO_3$ pellets sintered at 950 °C for 2 h in air. As shown in the micrographs, at this sintering temperature all the sintered pellets achieved sufficiently dense microstructure. The relative density of the sintered pellets was measured to be 96%.

3.3. Dielectric characterization of undoped and cation modified $LaFeO_3$ powders

Fig. 4 shows the temperature dependence of (a) dielectric constant and (b) loss tangent of (i) $LaFeO_3$, (ii) 10.0 at.%, and (iii) 20.0 at.% Pb doped pellets sintered at 950 °C for 2 h in air. We have identified that the dielectric maxima of $LaFeO_3$ systematically shift to higher temperature in $La_{0.9}Pb_{0.1}FeO_3$ and $La_{0.8}Pb_{0.2}FeO_3$ ceramics. Interestingly, for $La_{0.8}Pb_{0.2}FeO_3$ ceramics the temperature dependence resembles to that observed in typical colossal dielectric constant (CDC) ceramics [21]. To better understand this feature we have measured the frequency dependence of the dielectric constant and loss tangent of Pb doped $LaFeO_3$ ceramics in the temperature range of 300–500 K.

In the temperature range 300–500 K, Fig. 5 shows the frequency dependence of (a) the dielectric constant and (b) the loss tangent of (i) $LaFeO_3$, (ii) 10.0 at.%, and (iii) 20.0 at.% Pb doped pellets sintered at 950 °C for 2 h in air. As shown, Pb doped $LaFeO_3$ ceramics (Fig. 5(a) (ii) and (iii)) exhibit typical CDC like behavior. Thus, the CDC behavior is characterized by very high dielectric constant and lower frequency with a plateau like region followed by sharp drop in dielectric constant relatively at higher measurement frequencies. Summarizing the temperature and frequency dependence of the dielectric constant it can be stated that with lower *A* site dopant content (Pb^{2+} up to 10%), the dielectric maxima shift to higher temperature similar to that observed in ferroelectric material. With further increase in dopant contents, the Pb doped ceramics behaves like a CDC material.